Zinc Acetate Impact on AOA

Effective December 6, 2006, this report has been made publicly available in accordance with Section 734.3(b)(3) and published in accordance with Section 734.7 of the U.S. Export Administration Regulations. As a result of this publication, this report is subject to only copyright protection and does not require any license agreement from EPRI. This notice supersedes the export control restrictions and any proprietary licensed material notices embedded in the document prior to publication.

WARNING:
Please read the Export Control and License Agreement on the back cover before removing the Wrapping Material.

Zinc Acetate Impact on AOA

1001396

Technical Progress, February 2001

EPRI Project Manager

J. Deshon

EPRI • 3412 Hillview Avenue, Palo Alto, California 94304 • PO Box 10412, Palo Alto, California 94303 • USA
800.313.3774 • 650.855.2121 • askepri@epri.com • www.epri.com

DISCLAIMER OF WARRANTIES AND LIMITATION OF LIABILITIES

THIS DOCUMENT WAS PREPARED BY THE ORGANIZATION(S) NAMED BELOW AS AN ACCOUNT OF WORK SPONSORED OR COSPONSORED BY THE ELECTRIC POWER RESEARCH INSTITUTE, INC. (EPRI). NEITHER EPRI, ANY MEMBER OF EPRI, ANY COSPONSOR, THE ORGANIZATION(S) BELOW, NOR ANY PERSON ACTING ON BEHALF OF ANY OF THEM:

(A) MAKES ANY WARRANTY OR REPRESENTATION WHATSOEVER, EXPRESS OR IMPLIED, (I) WITH RESPECT TO THE USE OF ANY INFORMATION, APPARATUS, METHOD, PROCESS, OR SIMILAR ITEM DISCLOSED IN THIS DOCUMENT, INCLUDING MERCHANTABILITY AND FITNESS FOR A PARTICULAR PURPOSE, OR (II) THAT SUCH USE DOES NOT INFRINGE ON OR INTERFERE WITH PRIVATELY OWNED RIGHTS, INCLUDING ANY PARTY'S INTELLECTUAL PROPERTY, OR (III) THAT THIS DOCUMENT IS SUITABLE TO ANY PARTICULAR USER'S CIRCUMSTANCE; OR

(B) ASSUMES RESPONSIBILITY FOR ANY DAMAGES OR OTHER LIABILITY WHATSOEVER (INCLUDING ANY CONSEQUENTIAL DAMAGES, EVEN IF EPRI OR ANY EPRI REPRESENTATIVE HAS BEEN ADVISED OF THE POSSIBILITY OF SUCH DAMAGES) RESULTING FROM YOUR SELECTION OR USE OF THIS DOCUMENT OR ANY INFORMATION, APPARATUS, METHOD, PROCESS, OR SIMILAR ITEM DISCLOSED IN THIS DOCUMENT.

ORGANIZATION(S) THAT PREPARED THIS DOCUMENT

NWT Corporation

This is an EPRI Level 2 report. A Level 2 report is intended as an informal report of continuing research, a meeting, or a topical study. It is not a final EPRI technical report.

ORDERING INFORMATION

Requests for copies of this report should be directed to the EPRI Distribution Center, 1355 Willow Way, Suite 2478, Concord, CA 94520, (800) 313-3774.

Electric Power Research Institute and EPRI are registered service marks of the Electric Power Research Institute, Inc. EPRI. ELECTRIFY THE WORLD is a service mark of the Electric Power Research Institute, Inc.

Copyright © 2001 Electric Power Research Institute, Inc. All rights reserved.

CITATIONS

This report was prepared by

NWT Corporation
7015 Realm Drive
San Jose, CA 95119

Principal Investigator
S. G. Sawochka

This report describes research sponsored by EPRI.

The report is a corporate document that should be cited in the literature in the following manner:

Zinc Acetate Impact on AOA, EPRI, Palo Alto, CA: 2001. 1001396.

REPORT SUMMARY

The addition of zinc to PWR primary coolant has been suggested as a means for mitigating stress corrosion cracking of Alloy 600 and reduction of shutdown radiation fields. A further potential benefit of zinc addition could be amelioration of axial offset anomaly (AOA) at plants experiencing a large amount of corrosion product deposits on fuel. It is the purpose of this paper to estimate the beneficial effect, if any, of zinc addition on reducing the in-core fuel deposits, which are necessary for AOA to occur in high duty cores.

Background

Zinc acetate addition has been added to the reactor coolant during at least a portion of several fuel cycles at a number of PWRs. The focus of these additions has been mitigating stress corrosion cracking of Alloy 600 and reduction of shutdown radiation fields. The zinc is commonly added as the acetate salt, either in its natural form or using zinc depleted in the ^{64}Zn isotope. The aqueous zinc solution is conveniently added to the reactor coolant through the suction of the CVCS charging pump. Following a brief startup period, the zinc concentration is commonly controlled in the range of 5 to 40 ppb in the reactor coolant system.

Objective

To assess the possible impact of zinc injection to the PWR primary system on fuel cladding corrosion product deposition, and the potential benefit for mitigating AOA.

Approach

Laboratory data on the impact of zinc injection on corrosion and corrosion product release rates from primary system materials were reviewed. Estimations of core-average deposit magnitudes based on corrosion rates and corrosion product release rates have been met with reasonable success, and relatively simplistic models have provided valuable insights into deposit distribution in the core. Available corrosion product deposit and release rate data were then compared between PWRs injecting zinc and those not injecting zinc.

Results

Both corrosion and corrosion product release rates are observed to be reduced through zinc injection. Based on the reported reductions, significant reductions in average fuel deposit magnitudes appear achievable based on mass-balance considerations. Further, the small amount of plant data available on the effect of zinc on fuel deposits suggests that there is no detrimental effect of zinc on either deposit magnitude or its characteristics. End of cycle fuel inspections at Farley-2 also suggest that zinc injection has had no detrimental effect on fuel cladding corrosion.

Thus, there may be a benefit of zinc addition relative to reducing the tendency for AOA, but some residual questions remain.

EPRI Perspective

Addition of zinc to PWR primary coolant is expected to be beneficial for mitigating stress corrosion cracking. A further benefit is that low levels of depleted zinc oxide addition have been shown to reduce shutdown dose rates. This paper examines the additional effect of zinc in reducing the corrosion and release of corrosion products from ex-core surfaces. The observation that both rates are significantly reduced suggests that plants operating with zinc addition would experience a lower rate of corrosion product deposit growth on fuel, which would in turn reduce the tendency toward AOA.

Some cautionary issues should be addressed in evaluating zinc addition in PWRs, however. First, high Ni and ^{58}Co releases have been observed at shutdown following initial injection of zinc. Thus, zinc may increase the release of nickel and total deposit mass when first applied. This effect could exacerbate AOA for high duty plants that currently suffer from this problem. Secondly, zinc injection has not yet been used in a high duty AOA susceptible core, and it is not known whether this element will have an adverse impact on fuel deposits under conditions of high steaming rates. However, it should be noted that zinc addition has been practiced for many years at BWRs with no reported ill effects on either fuel deposits or cladding.

EPRI Product ID 1001396

Interest Categories

Fuel assembly reliability and performance
Robust Fuel Program
Water Chemistry
Radiation Exposure Management

Keywords

Axial offset anomaly (AOA)
Corrosion
Corrosion Product Transport
Fuel deposits

SUMMARY

To assess the possible impact of zinc injection to the PWR primary system on fuel cladding corrosion product deposit magnitudes and the tendency for developing a core axial offset anomaly (AOA), laboratory data on the impact of zinc injection on corrosion and corrosion product release rates of system materials were considered. Based on reported reductions in both corrosion and release rates, significant reductions in average fuel deposit magnitudes appear achievable with zinc injection based on mass balance considerations. In addition, fuel deposit data from Farley 2 indicate the absence of any significant detrimental effect on deposit magnitudes and characteristics, and Westinghouse concluded that zinc additions had no impact on fuel cladding corrosion based on a Farley 2 EOC13 inspection. However, data are limited, and Farley 2 only operated with zinc injection during the last 9 months of Cycle 10, 3 months of Cycle 12 and the last 10 months of Cycle 13. In addition, Farley 2 is not a high boiling duty plant. Although there may be a benefit of zinc injection relative to reducing the tendency for AOA, and risks currently appear modest, residual questions remain. For example, applicability of the laboratory corrosion data (taken during exposures only up to 2500 hours) to prediction of corrosion and release rates of surfaces filmed over periods of many years is open to discussion. In addition, increased nickel and Co-58 releases have occurred during shutdowns following operation with zinc and could negatively impact outage operations.

CONTENTS

LIST OF FIGURES

LIST OF TABLES

1
INTRODUCTION

Corrosion product deposition on PWR fuel cladding surfaces is of concern for several reasons. First, increases in cladding temperature and corresponding increases in Zircaloy oxidation rates can occur. Second, deposits in boiling regions can provide a matrix in which lithium borate solutions can concentrate possibly resulting in $LiBO_2$ precipitation or increased borate absorption which can cause local and regional flux depressions. Flux depressions (axial power offsets) can be sufficiently severe that full power operation may not be possible. Although early studies of deposits present on cladding surfaces subsequent to plant shutdown generally indicated that deposition of nickel iron ferrites was occurring, more detailed review of these data coupled with consideration of nickel releases during shutdown transients strongly indicates that current generation plant deposits contain significant amounts of nickel/nickel oxide as well as ferrites.

Attempts to estimate core average deposit magnitudes based on corrosion and corrosion product release rates of system materials (1-1) have been met with reasonable success, and relatively simplistic models have provided valuable insights with respect to deposit distribution (1-2) in the core. Conclusions of these efforts have been that variations in the lithium control (pH_T) methodology have only modest effects on deposition and that deposition rates increase as the extent of core boiling increases. Nonetheless, there is continued pressure to increase fuel exposures and fuel peaking factors and thus the extent of local boiling. Since laboratory data indicated that corrosion and release rates of system materials decrease in the presence of low zinc concentrations (e.g. 50 ppb), a limited review was performed to assess the impact of zinc acetate injection on average deposit magnitudes and compositions. Zinc acetate has been injected at several units for PWSCC mitigation and shutdown dose rate control.

References

1-1. Sawochka, S. G., “Impact of PWR Primary Chemistry on Corrosion Product Deposition on Fuel Cladding Surfaces,” Electric Power Research Institute, November 1997 (EPRI TR108783).

1-2. Fruzzetti, K. and Sawochka, S. G., “Modeling Deposit Formation on PWR Fuel Cladding Surfaces,” Light Water Reactor Fuel Performance Conference, Park City, Utah, April 2000.

2
CORROSION OF SYSTEM MATERIALS

Introduction

Based on mass balance considerations, it can readily be shown that corrosion product releases from PWR primary system materials control deposit buildup on fuel cladding surfaces. However, in attempting to quantify release rates at operating plants, several problems were encountered. First, laboratory data for corrosion and corrosion product release rates of Alloys 600, 690, and 800 and austenitic stainless steels varied markedly as a result of variations in test duration, pH, oxygen concentrations, coolant velocity, initial surface finish, etc. Second, laboratory results generally were obtained over relatively short times. Thus, such data yielded maximum values relative to expected equilibrium corrosion and corrosion product release rates in operating units since corrosion rates of the referenced materials decrease markedly with time at PWR primary coolant chemistry conditions

It also has been shown by Lister (Table 2-1) that the release rate from corroding surfaces is impacted by the corrosion product solution concentration relative to saturation. Lister (2-1), expressed this dependence in terms of equivalent alloy penetration based on release rate measurements for iron from stainless steel for assumed values of k_p, a precipitation kinetic constant for iron. At k_p=0, the solution has a negligible iron concentration and most of the iron is released into the coolant. If k_p=∞, surface precipitation has the maximum effect, the solution concentration approaches saturation, and minimal release occurs. Even through there is a major effect of coolant corrosion product concentration on metal release, Lister demonstrated that the stainless steel corrosion rate (Table 2-1) was independent of release and argued that the corrosion rate was controlled by a thin base layer of chromium-rich oxide. He suggested that Alloy 600 behavior would be similar although the short duration of his tests precluded obtaining sufficiently accurate data to confirm this point.

Corrosion and Release Rates in Non-Zinc Environments

Based on the premise that the at-temperature pH is the controlling parameter relative to the corrosion rate in zinc free environments, several approaches were previously employed by the author (2-2) in an attempt to develop correlations of laboratory corrosion and release rate data with pH_T. These approaches emphasized data from a single investigator at constant temperature, e.g., Figures 2-1 and 2-2. Although the general trends of the results were consistent over the pH_T (at-temperature pH) range covered, different dependencies were present in the range of interest (pH_T 6.9 to 7.4). Specifically, the corrosion rate results of Fletcher (2-3) for Alloy 600 indicated a minimal pH_T dependence, whereas the nickel release results of Beslu et al. (2-4) for Alloys 600 and 690 indicated a significant decrease with pH_T in the same temperature range. Corrosion and

release rates for stainless steel 304 (2-5) significantly decreased as pH_T was increased from 5.7 to 7.25, but only limited data at pertinent conditions and exposure times were available.

Recognizing such differences, a mixed approach was used to establish corrosion and release rate correlations for plant simulations (2-2). To develop the general dependence on pH_T, the results of Fletcher for Alloy 600 (2-3) were used (see Figure 2-1). However, as Fletcher pointed out, his average corrosion rates were expected to be significantly higher than in-plant values since his exposure times were only two to five months. On reviewing available corrosion rate data for Alloy 600 and 300 series stainless steels, a judgment was made that reasonable equilibrium values were on the order of 1 mg/dm^2-mo for Alloy 600 and 2 mg/dm^2-mo for stainless steel at a pH_T of 7.0 in the temperature range of 288 to 316^{o}C. On this basis, the correlation of Fletcher's data was normalized to yield the following corrosion rate estimates after the initial cycle of operation:

Alloy 600 Corrosion Rate:

$$CR_{600}=0.83(10^6)[H^+]+0.92$$

Stainless Steel Corrosion Rate:

$$CR_{SS}=1.7\,(10^6)[H^+]+1.84$$

Note that corrosion and corrosion product release rate reductions are expected for Alloy 600 and austenitic stainless steels as pH_T is increased. As a result, reductions in corrosion product deposition on fuel surfaces are expected as pH_T is increased. However, the achievable reduction is not particularly significant as pH_T is increased in the range of current interest.

Corrosion rate estimates based on the above relations are shown in Figure 2-3. The Alloy 600 relation leads to estimates of steam generator corrosion film growth rates consistent with reported values (2-6) as illustrated in Table 2-2, assuming only a fraction of the film is released.

In subsequent efforts to correlate fuel deposit data to corrosion rates, based on the above relations, release rates were expressed in terms of a release fraction (K_R):

Alloy 600 Release Rate:

$$RR_{600} = \left(0.83(10^6)(H^+) + 0.92\right)K_{R\,600}$$

Stainless Steel Release Rate:

$$RR_{SS} = \left(1.7(10^6)(H^+) + 1.84\right)K_{RSS}$$

Based on Lister's concept and the expected approach to saturated solution concentrations in the PWR, low values of the release fraction were expected, assuming that reasonable estimates of corrosion rates had been made. However, if primary coolant concentrations decreased

significantly below local saturation values, as a result of an increased rate of deposition on fuel cladding surfaces, metal release rates could increase even though corrosion rates would remain relatively constant.

Corrosion and Release Rates in Zinc Environments

The most complete set of data on corrosion and release rates from PWR primary system materials of construction in the presence of zinc appears to be that published by Esposito, et al., of Westinghouse Electric Corporation (2-7). The work of Lister (2-8) also was considered, but results were subsequently rejected from consideration (see Appendix A). In the Westinghouse study, coupons of 304SS, 316SS, Alloy 600 MA, Alloy 600 TT, Alloy 690 TT, Alloy 750, Zircaloy 4, Zirlo and Stellite were exposed at primary coolant conditions at 330°C in the presence and absence of zinc. Coupons were suspended in a four liter 316 SS vessel operated with a feedrate of approximately 300 cc/hour. The solution contained 1200 ppm boron and 2.2 ppm lithium (pH_T = 7.4). The hydrogen overpressure was maintained to produce 25 cc/kg in solution. During the zinc test, the autoclave inlet zinc concentration was 50 ppb. Zinc concentrations at the effluent were seldom above 20 ppb indicating significant zinc pickup by the autoclave and specimens over the course of the experiment.

Corrosion and metal release rate data in the presence and absence of zinc are summarized in Tables 2-3 and 2-4. Approximate corrosion and release rates over a 2500 hour (3.5 month exposure) are given in Table 2-5. The Table 2-3 and 2-4 data were used to develop the results of Table 2-6 in which the corrosion and release rates during various periods of exposure for 304 and 316 stainless steel, 600 MA, 600 TT and 690 TT are summarized. The ratio of the corrosion rates in the presence of zinc to those in the absence of zinc are shown along with a similar ratio for the release rates. In all cases, there was a significant reduction in both rates during zinc addition. The lower corrosion rates observed in the presence of zinc injection were supported by AES profiles of oxygen concentration on specimens exposed to zinc for 2500 hours and in the absence of zinc for 1300 and 2950 hours (Figure 2-4). As shown, the oxide films markedly decreased in the presence of zinc with the film thickness after 2500 hours being almost a factor of 5 lower than that observed on a specimen exposed for 2950 hours in the absence of zinc. AES profiles normalized to metals indicated incorporation of approximately 10% zinc at the coupon surface with detectable zinc concentrations observed 200 to 300 angstroms into the film (Figure 2-5). There also was an enrichment of nickel at the specimen surface in the absence of zinc injection compared to a depletion with zinc injection inferring a higher nickel to iron release ratio in the presence of zinc. Chrome depletion at the surface was evident in both cases.

To develop corrosion and release rate estimates for system materials in the presence of zinc, it appeared reasonable to rely on the ratios of Table 2-6 developed from the Esposito, et al. studies. Specifically, the average corrosion rate ratio during exposure to zinc compared to the absence of zinc was 0.36. Based on this data, preliminary relations for the corrosion rates of Alloy 600 and stainless steel in the presence of zinc were calculated from the non-zinc relations given above using a ratio of 0.4, i.e.:

$$CR_{600Z} = 0.33(10^6)[H^+] + 0.37$$

$$CR_{SSZ} = 0.68(10^6)[H^+] + 0.74$$

Although this approach is considered reasonable, it must be emphasized that the database with zinc addition was very limited, e.g.:

- Specimen exposure times were 2500 h or less
- All tests were done at one pH_T, and Li, B and H_2 concentrations at 300°C
- No plant data on film thickness were available for comparison to the above relations

References

2-1 Lister, D. H., "Corrosion-Product Release in LWRs: 1984-1985 Progress Report," Electric Power Research Institute, August 1986 (NP-4741).

2-2 Sawochka, S. G., "Impact of PWR Primary Chemistry on Corrosion Product Deposition on Fuel Cladding Surfaces," Electric Power Research Institute, November 1997 (EPRI TR-108783).

2-3 Fletcher, W. D., "Primary Coolant Chemistry of PWRs," Proc. 31st Intl. Water Conf., pp. 57-66, Pittsburgh, PA, October 1970.

2-4 Beslu, P. et al., "Elemental Release Rate Measurement of Inconel 600 and Inconel 690 in PWR Primary Coolant," Water Chemistry for Nuclear Reactor Systems, British Nuclear Energy Society, Bournemouth, October 1986.

2-5 Warzee, M., Sonnen, C., and Berge, Ph., "Corrosion of Carbon Steels and Stainless Steels in Pressurized Water at High Temperature," U.S. Atomic Energy Commission, July 1967 (EURAEC 1896).

2-6 Bergmann, C. A. and Roesmer, J., "Characterization of Primary Side Deposits in Pressurized Water Reactors," Corrosion 84 (Paper No. 194).

2-7 Esposito, J. N., et al., "The Addition of Zinc to Primary Reactor Coolant for Enhanced PWSCC Resistance,"

2-8 Lister, D. H., "The Effect of Dissolved Zinc on the Transport of Corrosion Products in PWR's," Electric Power Research Institute, September 1990 (EPRI NP-6975-D).

Table 2-1
Corrosion in Lithiated Coolant Saturated and Unsaturated in Corrosion Products (2-1)

Stainless Steel	Upstream Coupon - Saturated Coolant (nm penetration)	Downstream Coupon - Unsaturated Coolant (nm penetration)
Film Growth	180	40
Release	8	121
Total	188	161

Table 2-2
Data on Crud Removed from Selected Steam Generator Tube Films (2-7)

Plant	EFPY	Area Descaled, cm^2	Weight of Crud, mg	Surface Concentration, mg/dm^2	Apparent Density, gm/cm^3	Average Film Buildup Rates, mg/dm^2-mo
E	1.58	34.05	3.88	11.4	N/D[a]	0.60
B	1.75	31.71	4.04	12.7	N/D	0.60
D	2.21	31.47	6.07	19.3	N/D	0.73
			6.77[b]	21.5[b]	N/D	0.81
			7.38[c]	23.4[c]	N/D	0.88
G	5.96	32.25	15.44	47.9	3.99	0.67
			18.43[b]	57.1[b]	4.76[b]	0.80
			19.15[c]	59.4[c]	4.95[c]	0.83
G	6.84	35.86	11.94	33.3	3.92	0.40
			12.61[b]	31.5[b]	4.13[b]	0.42
A	7.02	31.89	13.86	43.5	3.81	0.52
			23.39[b]	73.3[b]	6.43[b]	0.82

a) Not determined
b) Includes a second descaling
c) Includes a third descaling

Table 2-3
Summary of Corrosion Data with Zinc Borate Addition (2-8)

Material	Exposure Time (hour)	Metal Loss (mg/dm^2)	Oxide Remaining (mg/dm^2)	Metal Release (mg/dm^2)
304 SS	500	1.70	1.81	0.43
304 SS	2500	3.75	4.77	0.41
316 SS	2500	4.34	5.53	0.47
600 MA	2500	6.66	7.50	1.42
600 MA	2500	3.77	4.43	0.66
600 TT	500	0.33	0.03	0.10
600 TT	1300	1.33	1.66	0.17
600 TT	2500	1.83	1.66	0.67
690 TT	500	0.50	1.00	-0.20
690 TT	1300	0.49	1.31	-0.40
690 TT	2500	0.81	1.93	-0.50
X-750	2500	2.00	1.87	0.69
STELLITE	800	1.98	1.85	0.69
	2500	3.68	3.82	1.00
	2500	1.22	1.22	0.37

Table 2-4
Summary of Corrosion Data without Zinc Borate Additions (2-8)

Material	Time (hour)	Metal Loss (mg/dm^2)	Oxide Remaining (mg/dm^2)	Metal Release (mg/dm^2)
304 SS	500	4.04	3.37	1.68
304 SS	2500	13.64	11.48	5.61
304 SS	2500	11.05	11.17	3.23
316 SS	2500	12.37	10.66	4.91
600 MA	500	4.26	5.41	0.47
600 MA	2500	7.61	7.46	2.39
600 MA	2500	10.49	10.32	3.27
600 MA	2500	10.83	10.33	3.60
600 MA	2500	6.88	6.39	2.41
600 TT	500	1.00	1.50	-0.05
600 TT	1300	6.66	6.66	2.00
600 TT	2500	7.16	5.83	3.10
690 TT	500	0.81	1.29	-0.09
690 TT	1300	3.28	3.44	0.87
690 TT	2500	4.50	3.33	2.17
X-750	2500	8.93	7.06	3.99
STELLITE	2500	61.80	16.00	50.60
	2500	74.90	25.50	57.10

Table 2-5
Approximate Corrosion and Corrosion Release Rates @ 3.5 Months (mg/dm^2/mo (MDM)) (2-8)

Material	Corrosion		Corrosion Release	
	with Zn	w/o Zn	with Zn	w/o Zn
304 SS	1.1	3.5	0.1	1.3
316 SS	1.3	3.5	0.1	1.4
600 MA	1.5	2.6	0.3	0.8
600 TT	0.5	2.1	0.2	0.9
690 TT	0.2	1.3	0.1	0.6
X-750	0.6	2.6	0.2	1.2
STELLITE	0.4	14.7	0.1	12.0

Table 2-6
Effect of Zinc Addition on Corrosion and Release Rates from PWR System Materials (a)

					Ratio Zn/No Zn	
Period	**Material**	**Zinc**	**Corrosion Rate, mg/dm2-mo**	**Release Rate, mg/dm2-mo**	**Corrosion Rate**	**Release Rate**
0-500 h	304 SS	N	5.94	2.47	0.42	0.26
		Y	2.5	0.63		
500-2500 h	304 SS	N	3.50	1.43	0.24	--
		N	2.56	0.56		
		Y	0.75	0		
0-2500 h	304 SS	N	3.99	1.64	0.30	0.09
		N	3.23	0.94		
		Y	1.10	0.12		
0-2500 h	316 SS	N	3.62	1.44	0.35	0.10
		Y	1.27	0.14		
0-500 h	600 MA	N	6.26	0.69		
0-500 h	600 TT	N	1.47	0	0.32	--
0-500 h	600 TT	Y	0.48	0.15		
0-500 h	690 TT	N	1.19	--	0.62	--
		Y	0.74	--		
0-2500 h	600 MA	N	2.22	0.7	0.58	0.35
		N	3.07	0.96		
		N	3.17	1.05		
		N	2.0l	0.70		
		Y	1.95	0.42		
		Y	1.10	0.19		
0-2500 h	600 TT	N	2.06	0.91	0.26	0.22
		Y	0.53	0.20		
0-2500 h	690 TT	N	1.32	0.63	0.18	--
		Y	0.24	--		
500-1300 h	600 TT	N	5.16	1.82	0.18	0.03
		Y	0.91	0.06		
1300-2500 h	600 TT	N	0.50	0.67	0.60	0.45
		Y	0.30	0.30		
1300-2500 h	690 TT	N	0.74	0.79	0.26	--
		Y	0.19	--		
			Average		0.36 ± 0.16	0.21 ± 0.15

a). Based on data from reference 2-8

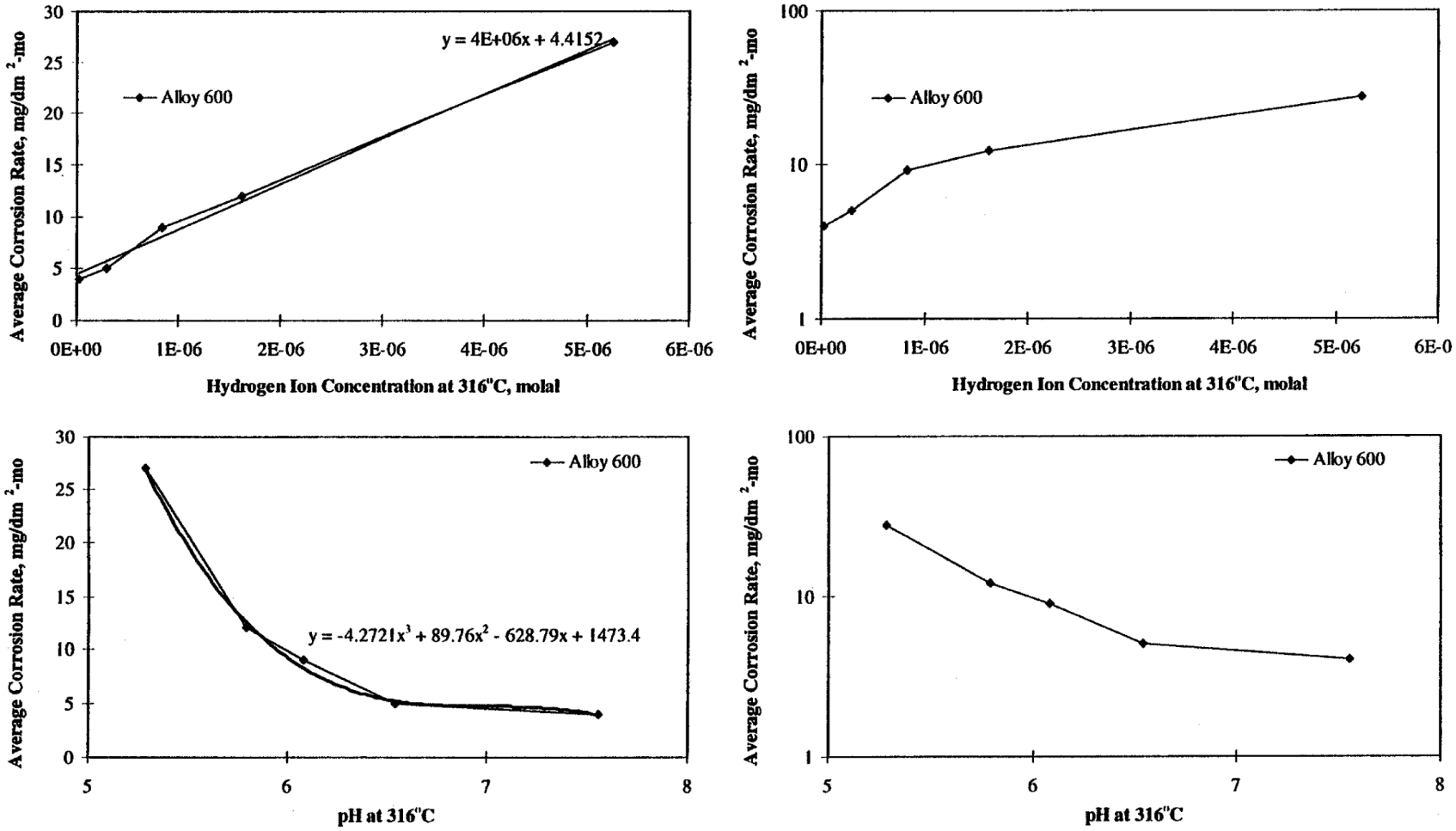

Figure 2-1
Relation of Average Alloy 600 Corrosion Rate to pH_T and Hydrogen Ion Concentration at 316°C (Reference 2-4 data: 2 to 5 month exposure)

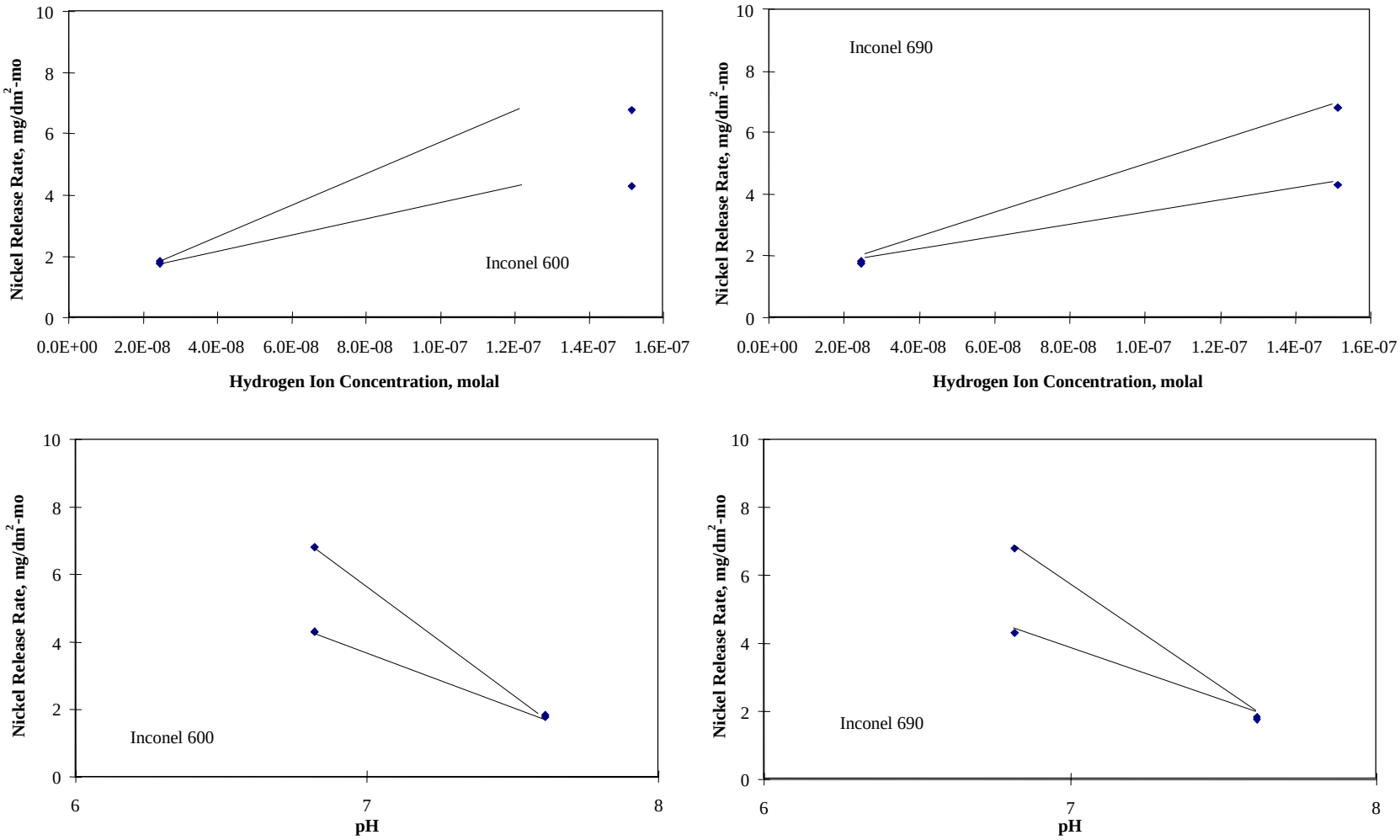

Figure 2-2
Relation of Alloy 600 Nickel Release Rate to pH_T and Hydrogen Ion Concentration at 320°C (Reference 2-5)

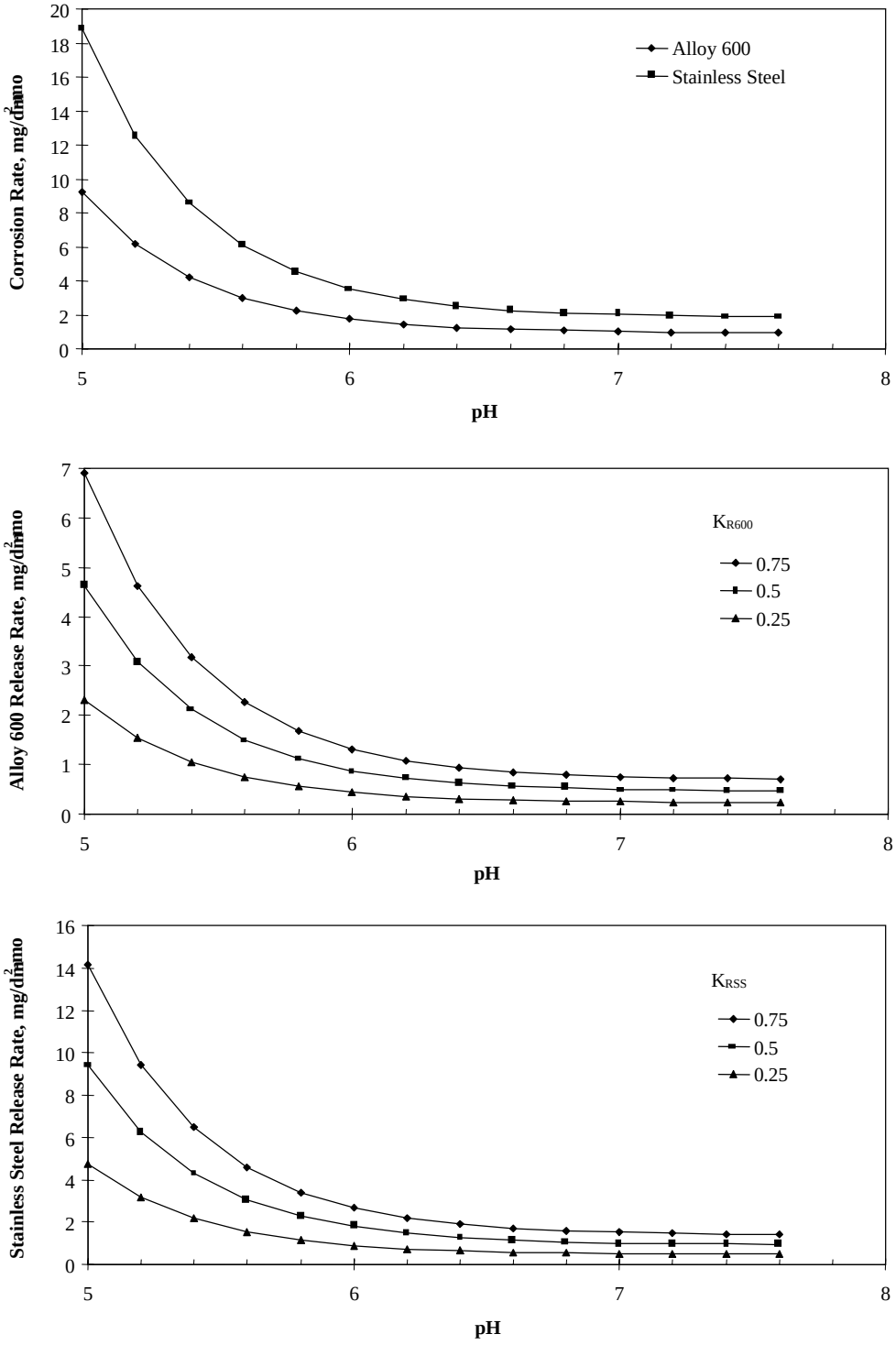

Figure 2-3
Estimated Corrosion Rates and Metal Release Rates for Alloy 600 and 300 Series Stainless Steel at 288 to 316ºC (Reference 2-3)

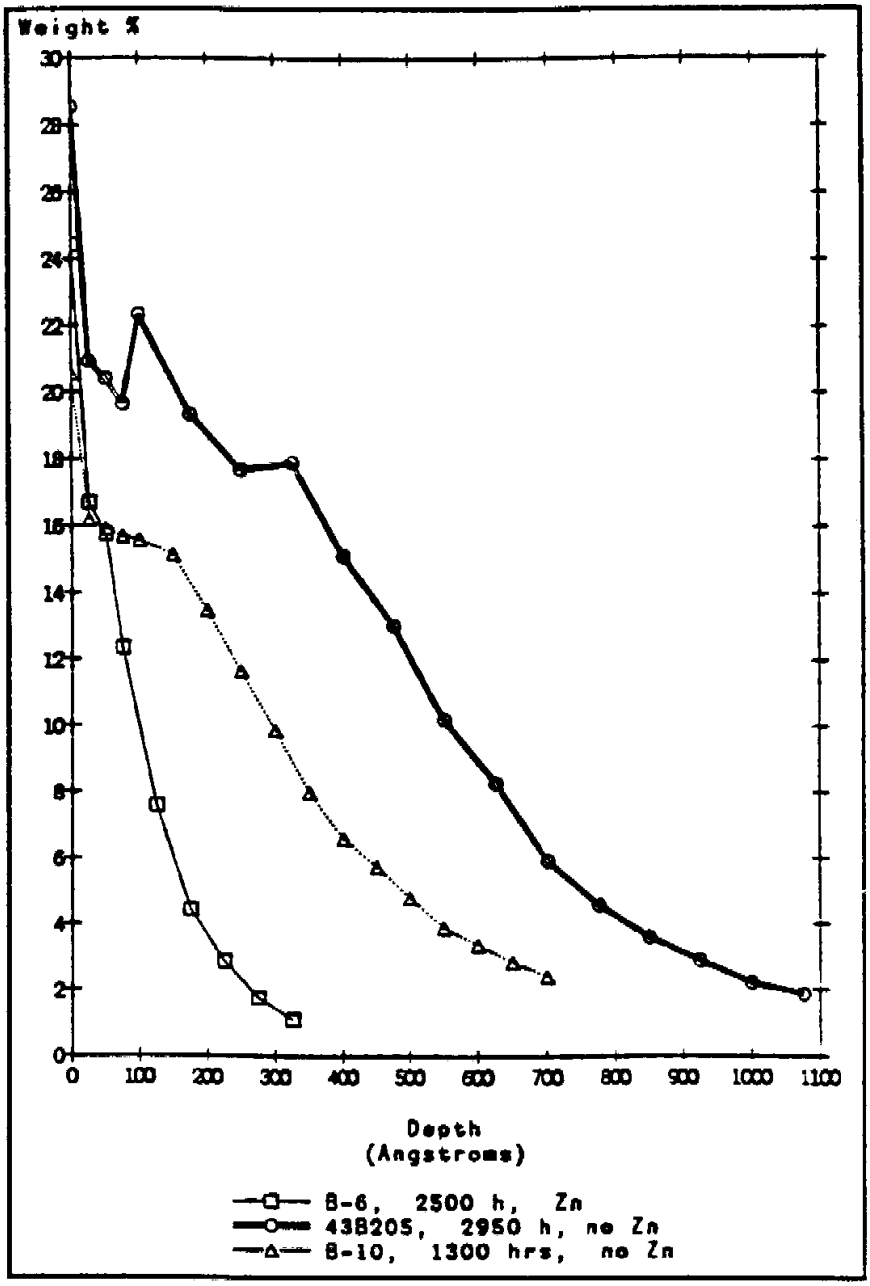

Figure 2-4
Comparison of AES profiles for oxygen on the surfaces of Alloy 600 MA specimens exposed to simulated primary coolant either with or Without zinc borate addition (Reference 2-8)

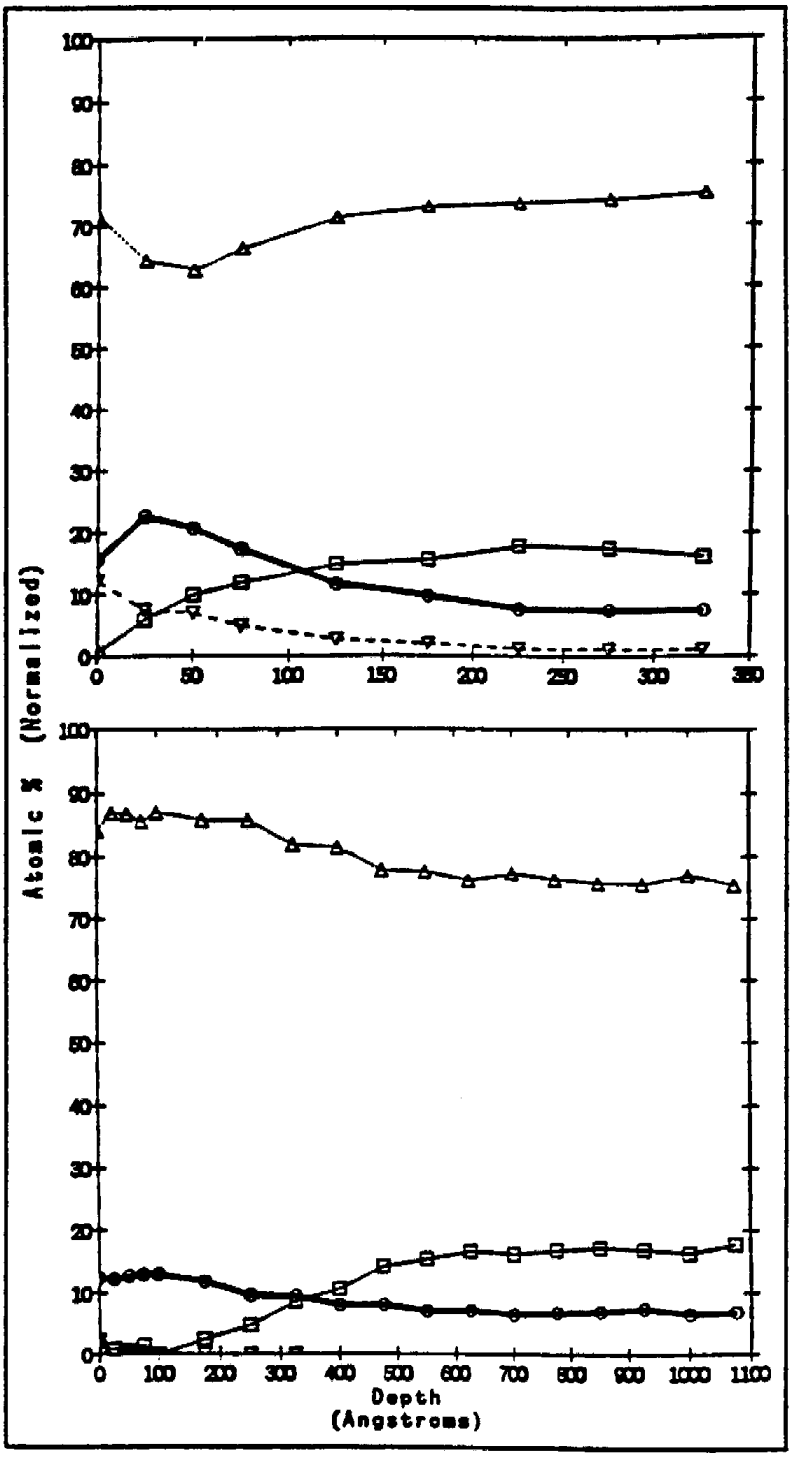

Figure 2-5
AES depth profiles for Alloy 600MA specimens exposed to simulated primary coolant with (a-upper) and without (b-lower) zinc borate (Reference 2-8)

3
CORROSION PRODUCT DEPOSIT MAGNITUDES

Numerous models have been proposed for predicting the rate of particulate deposition as well as precipitation on cladding surfaces. These models have varied from relatively simplistic (3-1) to very sophisticated (3-2, 3-3). In this effort, a simplistic "source term" approach was used to estimate average corrosion product deposit magnitudes on cladding surfaces for alternate lithium control (pH_T) methodologies. In concept, this approach has been applied by several investigators (3-4, 3-5). In this study, the approach was based on the corrosion and corrosion product release rate data summarized in Section 2 and was identical to that used previously by the author (3-6). The following relations were used to estimate Alloy 600 corrosion rates after completion of the first cycle of operation:

Alloy 600 Corrosion Rates:

$$\text{No Zinc} \quad CR_{600} = 0.83(10^6)[H^+] + 0.92$$

$$\text{Zinc} \quad CR_{600_Z} = 0.33(10^6)[H^+] + 0.37$$

Stainless Steel Corrosion Rates:

$$\text{No Zinc} \quad CR_{SS} = 1.7(10^6)[H^+] + 1.84$$

$$\text{Zinc} \quad CR_{SS_Z} = 0.68(10^6)[H^+] + 0.74$$

Alloy 600 Release Rates:

$$\text{No Zinc} \quad KR_{600} \; CR_{600}$$

$$\text{Zinc} \quad KR_{600_Z} \, CR_{600Z}$$

Stainless Steel Release Rates:

$$\text{No Zinc} \quad KR_{SS} CR_{SS}$$

$$\text{Zinc} \quad KR_{SS_Z} \, CR_{SSZ}$$

where:

CR_{600} = Alloy 600 Corrosion Rate (Total Metals), mg/dm^2-mo

CR_{SS} = Stainless Steel Corrosion Rate (Total Metals), mg/dm^2-mo

KR = Fraction of Corrosion Product Released

The basis of the "source term" approach to estimating corrosion product deposition on fuel cladding surfaces is a mass balance for the primary system. Specifically, corrosion product release from the corroding surfaces minus the removal by the primary coolant purification system must equal the corrosion product mass deposited on the fuel cladding surfaces plus redeposition of released corrosion products on steam generator and piping surfaces, i.e.:

Corrosion Product Release - Purification System Removal = Deposition on Fuel Surfaces + Deposition on Other Primary System Surfaces

An estimate of the maximum fuel surface deposit magnitude assuming uniform deposition can be made by neglecting deposition on other than cladding surfaces and neglecting purification system removal, i.e., equating fuel surface deposition to total corrosion product release, i.e.:

$$\text{Maximum Average Deposit Magnitude} = \frac{\text{Corrosion Product Release}}{\text{Fuel Area}}$$

An example of the source term approach to estimating the maximum average corrosion product deposit magnitudes on fuel cladding surfaces in the absence of zinc is given below for a Westinghouse 1095 MW four loop plant operating at pH_T 7.0.

pH_T = 7.0 at T_{avg} (assumed constant over cycle)

CR_{600} = Alloy 600 Corrosion Rate = 1 mg/dm^2-mo

K_{R600} = 0.5 (assumed)

RR_{600} = Alloy 600 Release Rate = 0.5 mg/dm^2-mo

CR_{SS} = Stainless Steel Corrosion Rate = 2 mg/dm^2-mo

K_{RSS} = 0.5 (assumed)

RR_{SS} = Stainless Steel Release Rate = 1 mg/dm^2-mo

Zircaloy Fuel Area = $7.24(10^5)$ dm^2 (see Table 3-1)

Stainless Steel Area = $2.75(10^5)$ dm^2

Alloy 600 Area = $1.87(10^6)$ dm^2

Assumed Cycle Length = 15 months (~450 days)

Metal Release = $1.87(10^6)(0.5)(15)+2.75(10^5)(1)(15)$

= $1.81(10^7)$ mg = 18.1 kg

Avg. Surface Concentration = $\frac{18.1 \text{ kg}}{7.24(10^5)\ dm^2}$

= 25 mg/dm^2 as metals

= 34.4 mg/dm^2 as oxide (M_3O_4)

Using the above approach, maximum average corrosion product deposit magnitudes on fuel surfaces can be estimated for any lithium control strategy based on the corrosion rate correlations and assumed release fractions. (Approximate surface areas for several plant designs are given in Table 3-1.)

For example, predictions of maximum average corrosion product deposit magnitudes for a release fraction of 0.5 were developed for the following chemistry control options applied over a 15 month cycle at a Westinghouse 1095 MWe plant at a zinc and non-zinc plant:

Option A: Initial B = 1300 ppm; Linear boron decrease with time; constant 2.2 ppm lithium to pH_T = 7.4 then Li coordinated to maintain pH_T 7.4

Option B: Initial B = 1300 ppm; Linear boron decrease with time; Lithium controlled to maintain pH_T 6.9 at beginning of cycle until Li reduced to 2.2 ppm. Constant 2.2 ppm lithium to pH_T 7.4 then lithium gradually reduced to maintain pH_T 7.4.

Option C: Initial B = 1300 ppm; Linear boron decrease with time; Li controlled to maintain pH_T=6.9 throughout cycle.

Option D: Initial B = 1300 ppm; Linear boron decrease with time; Li controlled to maintain pH_T=6.7 throughout cycle.

As shown in Table 3-2, a significant reduction in deposit magnitudes is predicted with the use of zinc. However, only a small change in magnitude occurs for the above lithium/boron control methodologies, i.e., the total deposit is predicted to vary from approximately 24 kg to 27 kg at

non-zinc plants and 10 kg to 11 kg at zinc plants. This corresponds to an average deposit magnitude of 34 to 37 mg/dm^2 on 1 cycle fuel assuming uniform distribution on all fuel surfaces at non-zinc plants. If non-uniform deposition occurs, as normally is observed, local deposit magnitudes will increase. For example, if deposition occurs only on the upper 15% of the bundles at a non-zinc plant, the predicted deposit magnitudes increase to 230 to 260 mg/dm^2. At a zinc plant, this magnitude is predicted to decrease to approximately 100 mg/dm^2.

Note that removal of corrosion products from the primary coolant by the letdown purification system will reduce the amount of material available for deposition and thus reduce the amount of deposition on the fuel for a given release fraction. For example, at a purification system flowrate of 2.3(10^4) kg/h (100 gpm) and an average RCS concentration of 10 ppb, 2 kg/year (4.4 lbs/yr) will be removed by purification. This corresponds to 7% to 8% of the total release for a non-zinc plant and 14 to 16% at a zinc plant for the above four chemistries at an assumed release fraction of 0.5.

References

3-1 Lindsay, W. T., Jr., "CRUD-SIM: Semi-Empirical Approach to Statistical Modeling" Westinghouse Electric Corporation, 1985.

3-2 "Primary Side Deposits on PWR Steam Generator Tubes," Electric Power Research Institute, March 1983 (NP-2988).

3-3 Beslu, P., Frejaville, G., and Lalet, A., "A Computer Code PACTOLE to Predict Activation and Transport of Corrosion Products in a PWR," British Nuclear Energy Society, International Conference on Water Chemistry of Nuclear Reactor Systems, Bournemouth, England, October 1977.

3-4 Polley, L. V. and Pick, M. E., "Iron, Nickel and Chromium Mass Balances in Westinghouse PWR Primary Circuits," Water Chemistry for Nuclear Reactor Systems, British Nuclear Energy Society, Bournemouth, October 1986.

3-5 Roesmer, J. and Rootham, M. W., "Estimation of Activity Inventories in Primary Circuits of Pressurized Water Reactors," International Conference on Water Chemistry, Bournemouth, England, October 1977 (Paper 22).

3-6 Sawochka, S. G., "Impact of PWR Primary Chemistry on Corrosion Product Deposition on Fuel Cladding Surfaces," Electric Power Research Institute, November 1997 (EPRI TR-108783).

Table 3-1
Major Surface Areas and Materials in Typical Westinghouse, ABB-CE and B&W Plants

Surface Area, dm^2 (% of total)

Material	Fuel Assembly Surfaces	In-Vessel Non-Fuel Surfaces	Ex-Vessel Surfaces	Inconel + SS Fuel
W 810 MW (Three Loop) Plant				
Stainless Steel	14,500 (0.7)	158,900 (7.1)	64,700 (2.9)	2.95
Inconel	58,200 (2.6)	3,100 (0.1)	1,345,000 (61.1)	---
Zircaloy-4	558,000 (25.3)	---	---	---
W 1095 MW (Four Loop) Plant				
Stainless Steel	17,500 (0.6)	175,000 (6.1)	83,300 (2.9)	2.96
Inconel	72,800 (2.5)	3,200 (0.1)	1,793,000 (62.5)	---
Zircaloy-4	724,000 (25.2)	---	---	---
ABB-CE 860 MW (Two Loop) Plant				
Stainless Steel	11,400 (0.5)	131,900 (5.8)	34,500 (1.5)	2.85
Inconel	---	19,000 (0.8)	1,487,000 (65.3)	---
Zircaloy-4	590,800 (26.0)	---	---	---
B&W FA 177 Plant				
Stainless Steel	66,800 (2.3)	71,000 (2.4)	80,200 (2.8)	5.27
Inconel	---	71,200 (2.5)	2,140,000 (74.0)	---
Zircaloy-4	461,000 (16.0)	---	---	---

Table 3-2
Predicted Corrosion Product Deposit Magnitude on One Cycle Fuel at a Westinghouse 1095 MWe Plant (450 day cycle)[a]

	Total Release, Kg		Corrosion Product Deposit, mg/dm^2	
	Non-Zinc Plant	Zinc Plant	Non-Zinc Plant	Zinc Plant
Uniform Deposition				
2.2 ppm Li/pH_T 7.4	24	9.6	34	14
pH_T 6.9/2.2 ppm Li/pH_T 7.4	24	9.6	34	14
pH_T 6.9	25	10	35	14
pH_T 6.7	27	10.8	37	15
Localized Deposition[b]				
2.2 ppm Li/pH_T 7.4	24	9.6	234	94
pH_T 6.9/2.2 ppm Li/pH_T 7.4	24	9.6	2345	94
pH_T 6.9	25	10	245	98
pH_T 6.7	27	10.8	260	104

a. Applies only after initial cycle of operation (subsequent to filming primary system surfaces); values are for M_3O_4 oxide; release fraction of 0.5

b. Deposition on 15% of fuel cladding surface

4
FUEL DEPOSIT MAGNITUDES AND CORROSION PRODUCT RELEASE FRACTION

Non-Zinc Environments

In Reference (4-1), predictions of average corrosion product deposit magnitudes as a function of the release fraction were developed for non-zinc plants for which deposit data were available, and the predictions and observations were compared to develop estimates of release fractions. Results for Cycle 10 at Farley 2, where zinc was injected during the last 9 months of the cycle, were also considered. To correct the observed deposit values for releases during shutdowns, plant data were used where available. When data were not available, a release of 4.1 kg of NiO and 0.4 kg of Fe_3O_4 was estimated for an 1150 MWe plant. Releases were proportionally reduced for lower power units. This release corresponds to an average deposit magnitude of approximately 6.2 mg/dm^2 at an 1150 MWe plant, which is significant with respect to the total deposit magnitude observed at many of the study plants during post-shutdown fuel scraping efforts. In fact, the predicted release exceeded the residual deposit magnitude in about 50% of the study cases.

To correct the total release values for purification system removal during normal operation, average primary coolant iron and nickel concentrations of 2 ppb and 1 ppb, respectively, were assumed. At an average purification rate of 1.8(10^4) kg/h (80 gpm), and a cycle length of 12 months, a removal of 0.65 kg per cycle of M_3O_4 was estimated. This corresponds to a uniformly distributed deposit of 0.9 mg/dm^2 for an 1150 MWe unit and 1.3 mg/dm^2 for an 800 MWe unit. Corrections for cycle length and primary coolant concentration deviations from the indicated estimates were not attempted.

A value of the release rate constant for stainless steel and Alloy 600 (equal values were assumed) was then calculated from the corrosion product mass balance and the observed average deposit magnitude. Results are summarized in Table 4-1 (4-1). The average release fraction was 0.20 ± 0.10. The low value is consistent with expectations assuming the primary coolant remains near saturation at the average primary coolant temperature. Recognizing the limited database that was available, and the scatter in the deposit data, the consistency of the release fraction estimates is considered reasonable. Of particular note is the consistency of the Farley 2 Cycle 9 and 10 results which infers the absence of a significant impact of zinc on corrosion product release fraction.

Other than the results for Trojan Cycle 1 where operation at a much lower pH than currently recommended led to an apparent release rate fraction of >0.4, the only other fuel with a deposit magnitude consistent with a release rate fraction of >0.4 was Callaway two cycle fuel at the end

of Cycle 6. Since the chemistry control program at Callaway during Cycles 5 and 6 did not differ significantly from those at plants exhibiting apparent release rate fractions of 10 to 20%, this infers that non-chemistry related factors or high-side biases in the deposit data are the cause of the deviation from the norm. In this regard, it should be noted that the mass evaporation rate in subcooled nucleate boiling regions at Callaway during Cycle 5 has been reported to be the highest of any cycle considered by Westinghouse during a recent review of axial power offset anomalies (4-2). The Cycle 6 mass evaporation rate was the third highest of the study plants. Note that concentration of ionic corrosion products within deposits in boiling regions increases the tendency for preferential deposition in these regions and also could decrease primary coolant soluble concentrations at the core outlet below saturation thereby increasing release rates from Alloy 600 and stainless steel (4-3). Either or both of these effects would be consistent with observation of a much higher than average apparent release rate at Callaway during Cycles 5 and 6.

Zinc Environments

Fuel deposit data following operation with zinc are very limited. Specifically, deposit data (other than visual) only are available for Farley 2 (EOC 10). Farley 2 operational history with zinc is as follows:

- Zinc was injected for the last nine months of Cycle 10; the estimated net accumulation in the RCS was 3.83 kg Zn.
- Zinc addition was suspended during Cycle 11 pending root cause evaluation of fuel cladding oxidation seen at EOC 10.
- Zinc was added to the RCS for 3 months in the middle of Cycle 12; the estimated net mass of zinc added this cycle was 1.03 kg.
- Zinc was added to the RCS for the last 10 months of Cycle 13; the estimated net mass of zinc added during this cycle was 2.31 kg.

A summary of fuel assemblies from which deposit samples were obtained at Farley 1 and 2 is given in Table 4-2. Deposit data are given in Tables 4-3 and 4-4. Results can be summarized as follows:

1. Deposit magnitudes on once burned Farley 2 fuel at EOC 9 (no zinc) and EOC 10 (9 months on zinc) were very similar in span 6. However, slightly lower deposit magnitudes were observed at EOC 10.

2. No significant increase in deposit magnitude occurred on once and twice burned Cycle 9 fuel exposed during Cycle 10.

3. Zinc incorporation into the deposit was minimal, i.e., 2 to 4% of deposit weight.

4. Farley 1 deposit magnitudes on Cycle 13 feed fuel were approximately 10 times greater than observed on Farley 2 Cycle 9 and 10 feed fuel. Westinghouse attributed this

difference to coolant chemistry. However, deposit magnitudes on Unit 1 twice burned fuel (Cycles 12 +13) were consistent with Unit 2 twice burned fuel (Cycles 9 + 10).

In summary, there appears to have been no significant effect of zinc on deposit magnitudes. In fact, Westinghouse concluded that "the addition of Zn to the coolant of a PWR may lead to a small reduction in crud thickness."

Only visual observations were made at Farley 2 at EOC 11. Westinghouse summarized the findings as follows: (4-4):

The crud burden on the fuel rods was generally quite small; there was very little crud on the rod surfaces with most of the crud present as a light uniform coating. Only a few spans had dark, non-reflective crud.

On most of the once and twice burned assemblies there was a light uniform layer of non-reflective crud or dark oxide on the first span. The second spans typically showed a mottled oxide appearance. Similar features were seen on rods in the third span and appeared to be a transition between the oxide and a dark shiny (reflective) uniform coating over the oxide which began to appear on the rod surfaces in the second and third spans. This shiny coating extended to the middle of the top span in both the once burned and twice burned assemblies. This coating had a shiny metallic appearance, indicative more of cladding oxide than crud, and was sufficiently thin that scratches could be seen on the rod surface. The reflective coating appeared slightly darker in the twice burned "2M" assemblies.

For comparison, videos of fuel assemblies taken at the EOC 10 outage were reviewed and contrasted with those from the EOC 11 inspections. All of the EOC 10 fuel assemblies were covered with a dark coating which extended along the entire length of the assemblies from the bottom nozzle to the top nozzle. In the bottom three spans the coating was typically very dark and nonreflective. In the higher spans, the coating was still dark in color cut was slightly reflective, and became increasingly reflective with elevation.The amount of coating appeared to vary with assembly burnup. The once burned assemblies appeared to have the most crud and the thrice burned assemblies the least. In some of the assemblies, areas near the grids and IFMs had a pattern of patches and streaks of crud rather than a uniform coating.

The EOC 10 rods were much darker in appearance than the EOC 11 rods and significantly more crud was present, being especially prevalent in the bottom three spans of the EOC 10 assemblies. In the higher spans where both sets of assemblies had a generally shiny appearance, the EOC 11 rods were much brighter than the EOC 10 rods, with very little evidence of crud.The shiny coating on the EOC 10 rods was much darker in color, and was only slightly reflective, compared to the EOC 11 rods.

A direct comparison was made of the appearance of fuel assembly 2M56 at the EOC 10 (once burned) and EOC 11 (twice burned) outages. The differences in appearance are accurately described above. The videos also showed that in the areas where the assembly had patches or streaks of crud,the pattern was similar after both cycles.

At EOC 13, after 10 months of zinc injection, the following observations were reported (4-5):

"*Visual inspection of the surfaces of the measured fuel rods/assemblies during the refueling operations indicated that the rods were covered with a dark semi-reflective coating. This coating was similar in appearance to that seen at the end of virtually all fuel cycles following extended operation with zinc injection. This dark, semi-reflective coating is very thin, and has no appreciable effect on the oxide thickness measurements.*

Analysis of the Cycle 13 data, and comparison with other data for Improved Zircaloy-4 and ZIRLO™, indicates that zinc additions had no impact on the fuel cladding corrosion.

References

4-1 Sawochka, S. G., "Impact of PWR Primary Chemistry on Corrosion Product Deposition on Fuel Cladding Surfaces," Electric Power Research Institute, November 1997 (EPRI TR-108783).

4-2 Sabol, G. P., et al., "Rootcause Investigation of Axial Power Offset Anomaly," Electric Power Research Institute, June 1997 (TR-108230).

4-3 Lister, D. H., "Corrosion-Product Release in LWRs: 1984-1985 Progress Report," Electric Power Research Institute, August 1986 (NP-4741).

4-4 Gold, R. E., et al., "End-of-Cycle 11 Examinations at Farley Unit 2," Electric Power Research Institute, July 1997 (EPRI TR-107904).

4-5 Gold, R. E., et al., "Evaluation of Zinc Addition to the Primary Coolant of PWRs," Electric Power Research Institute, November 1996 (EPRI TR-106358-V1)

Table 4-1
Calculated Corrosion Product Release Fraction to Achieve Agreement Between Predicted and Observed Average Deposit Magnitudes

			Average Corrosion Product Deposit Weight, mg/dm^2	
Plant	**EOC**	**Fuel Status**	**Observed (Plant Data)**	**Calculated Release Fraction**
Beaver Valley 1	1	1 Cycle	14	0.11
Callaway	6	1 Cycle	9.1	0.22
		2 Cycle	55	0.48
		3 Cycle	20.5	0.19
Farley 1	13	1 Cycle	11.8	0.25
		2 Cycle	2.4	0.11
Farley 2	9	1 Cycle	3.1	0.14
		2 Cycle	1.5	0.11
		3 Cycle	1.5	0.11
Farley 2	10	1 Cycle	1.8	0.13
		2 Cycle	2.5	0.12
		3 Cycle	0.9	0.11
Millstone 3	2	1 Cycle	4.0	0.19
		2 Cycle	20.3	0.18
Millstone 3	4	1 Cycle	15.0	0.28
Plant A	2	1 Cycle	7.1	0.30
Plant A	4	1 Cycle	2.9	0.19
Trojan	1	1 Cycle	73	0.43
Trojan	2	1 Cycle	7.9	0.32
		2 Cycle	24.1	0.16
Trojan	3	1 Cycle	1.2	0.21
		2 Cycle	2.2	0.19
		3 Cycle	29.2	0.18
Tsuruga 2	4	2 Cycle	1.0	0.12

Table 4-2
Summary of Operational Details of the Sampled Assemblies (4-5)

Assembly	Unit	Cycles Operated	Rel. Power in Prior to Last Cycle	Rel. Power in Last Cycle
2E11	1	13	-----	1.27
2D29	1	12, 13	1.19	1.23
2L02	2	9, 10	1.06	1.05
2L26	2	9, 10	1.26	1.01
2L51	2	9, 10	1.29	1.01
2M19	2	10	-----	1.42
Y04	2	8, 9, 10	1.15	0.94
Y09	2	8, 9		1.16
Y47	2	8, 9, 10	1.16	1.00
W50	2	7, 8, 9		1.04
R48	2	3, 4, 9		1.00

Table 4-3
Comparison of Crud Thicknesses for Farley Unit 1 and Before and After Zinc Addition to Farley Unit 2 (4-5)

Span	Before Zinc Addition			After Zinc Addition		
	Cycle(s)	Surf. Conc'n., mg/dm²	Thickns., μm	Cycle(s)	Surf. Conc'n., mg/dm²	Thickns., μm
FARLEY UNIT 2						
	Assemblies 2L26, 2L51			Assembly 2M19		
6A	9	6.9 ± 1.1	0.57	10	4.3 ± 0.9	0.36
6B	9	4.1 ± 1.0	0.34	10	2.8 ± 0.4	0.24
6 (A+B)	9	5.0 ± 1.8	0.42	10	3.6 ± 1.2	0.30
				Assys. 2L02, 2L26, 2L51		
6 (A+B)	No Data Available			9, 10	5.5 ± 2.0	0.46
	Assembly Y09					
6	8, 9	2.6 ± 0.5	0.22	No Data Available		
	Assembly Y47			Assembly Y04		
5	8, 9	1.0 ± 0.1	0.10	8, 9, 10	1.3 ± 0.1	0.11
6	8, 9	1.9 ± 0.5	0.16	8, 9, 10	1.8 ± 0.3	0.15
FARLEY UNIT 1						
	Assembly 2E11					
6A	13	40	3.4			
6B	13	72	6.0			
6 (A+B)	13	56 ± 16	4.7			
	Assembly 2D29					
6A	12, 13	8.5	0.70			
6B	12, 13	7.3	0.61			
6 (A+B)	12, 13	7.9 ± 0.6	0.66			

Error indicators are standard deviations or differences between average and measured values in the case of only two determinations. Error indicators for thicknesses are not listed.

Table 4-4
Comparison of Average Crud Compositions on Span 6 (4-5)

	Once-Burned Fuel			Twice-Burned Fuel		
Unit/Cycle	2 / 9	2 / 10	1 / 13	2 / 9	2 / 10	1 / 13
Assemblies	2L51, 2L26	2M19	2E11	Y09, Y47	2L26, 2L02, 2L51	2D29
Element	Chemical Concentration in Weight Percent ±					
Fe	43.6 ± 3.2	33.6 ± 3.6	38.3 ± 0.4	45.9 ± 2.7	35.0 ± 1.5	32.0 ± 1.1
Ni	21.4 ± 2.2	26.5 ± 4.8	29.8 ± 0.4	12.3 ± 1.0	21.6 ± 2.8	30.2 ± 1.3
Cr	7.2 ± 0.9	8.3 ± 0.4	5.2 ± 0.1	9.1 ± 0.5	9.3 ± 0.8	8.8 ± 2.0
Co	0.06 ± 0.02	0.30 ± 0.14	0.05 ± 0.02	0.04 ± 0.01	0.20 ± 0.04	0.06 ± 0.01
Zn	0.08 ± 0.04	2.43 ± 0.52	0.12 ± 0.01	0.09 ± 0.05	3.34 ± 0.59	0.18 ± 0.15
Cu	0.68 ± 0.23	0.93 ± 0.30	0.08 ± 0.03	1.32 ± 0.14	0.67 ± 0.19	0.50 ± 0.22
Al	0.10 ± 0.11	0.44 ± 0.59	0.03 ± 0.01	0.06 ± 0.02	0.72 ± 0.50	0.03 ± 0.01
Ca	0.12 ± 0.09	0.57 ± 0.74	0.09 ± 0.08	0.11 ± 0.03	0.78 ± 0.97	0.03 ± 0.01
Mg	0.08 ± 0.04	0.10 ± 0.05	0.05	0.14 ± 0.05	0.09 ± 0.11	0.03
Li	0.01 ± 0.01	<0.02	0.02 ± 0.01	0.01 ± 0.01	0.04 ± 0.02	0.03 ± 0.02
Ni/Fe	0.49 ± 0.07	0.81 ± 0.25	0.78 ± 0.02	0.27 ± 0.37	0.62 ± 0.10	0.92 ± 0.01

A
APPENDIX A

In an attempt to expand the database on the corrosion and release rate characteristics of Alloy 600 and stainless steels in the presence of zinc, the work of Lister was reviewed (A-1). In Lister's tests, two experiments were performed. Chemistry during Phase I and Phase 2 is summarized in Table A-1. Two Alloy 600 test sections were run in parallel with the test sections exposed alternately to periods of zinc injection and no zinc. The zinc concentration variations during Phase 1 are summarized in Figure A-1. In addition to the significant zinc concentration variations during the test, the high temperature pH of the coolant also varied markedly (Figure A-2). The on/off zinc sequencing during the experiment, the pH variations and the expected variations in corrosion and release rates with time markedly complicated the interpretation of Lister's results. In addition, Lister eventually concluded the Phase 1 results were anomalous and effectively disregarded these major results. In particular, corrosion film thicknesses increased more rapidly in the presence of zinc than they did in the absence of zinc during individual exposure periods and over the entire exposure period which was approximately 1554 hours. The oxide film thickness variations of Inconel 600 are summarized in Figure A-3. Film thickness estimates developed by AECL and the University of Western Ontario (UWO) are shown. From these results, estimates of film growth rate were developed for each exposure period (Table A-2). The lack of a significant beneficial effect of zinc on film growth is apparent as is a reduction in film growth rate as a function of time. Note, however, that during interpretation of these results it must be noted that the pH was gradually increasing during the 1554 hour test program (reference Figure A-2).

An attempt was also made to develop corrosion release rate estimates from the Co-58 release rates from activated specimens exposed to the same environment (Figure A-4). Results are summarized in Table A-3. A gradual reduction in the release rate from each test section with time is apparent. However, a modest benefit of zinc injection appears to be present when results for Test Sections 1 and 2 are compared during the same period of operation. Comparison of Table A-2 results for rate of film growth with the release rate (or equivalent penetration rate) estimates of Table A-3 suggests that a significant fraction of the film was released.

During Phase 2, zinc concentrations were better controlled (Figure A-5). However, the high temperature pH again varied markedly over the 2000 hour program (Figure A-6). Phase 2 results for oxide film thicknesses on Inconel 600 are summarized in Figure 3-7 and Table A-4. Although results vary markedly during different exposure periods, there appears to be a general trend of reduced film thickness during exposure to zinc. However, a coupon that had been exposed in Phase 1 for 500 hours with continued exposure at similar zinc conditions during Phase 2 to give a cumulative exposure of 2500 hours again indicated a negative impact of zinc on film thickness. It should be noted that if it is assumed that if there is minimal loss of corrosion products over the 2000 hour exposure period, an average corrosion rate on the order of 0.1

mg/dm^2-mo is calculated for the zinc case with a corresponding value of 0.5 mdm in the absence of zinc. Both of these values are significantly lower than would be expected based on results of other experimenters during an initial exposure of a clean non-filmed specimen.

Results for stainless steel are summarized in Table A-5. In this case, the average corrosion rate based on Lister's assumptions are near expected values for a 2000 hour exposure. The beneficial effect of zinc on the average corrosion rates appears to be on the order of a factor of 1.7. Results for the tracer concentration decrease in the activated specimen were not presented for this phase of the program thus the rate of release during Phase 2 could not be estimated.

In summary, Lister's results do not appear to provide a reliable database on corrosion and release rates of stainless steel or Inconel 600 when exposed to a typical PWR environment as a function of coolant zinc concentration.

References

A-1 Lister, D. H., "The Effect of Dissolved Zinc on the Transport of Corrosion Products in PWR's," Electric Power Research Institute, September 1990 (EPRI NP-6975-D).

Table A-1
Coolant Conditions During Release Experiment (A-1)

COOLANT CONDITIONS DURING RELEASE EXPERIMENT - PHASE 1

	TS 1	TS 2
Temperature (°C)	300	305
Flow Rate ($mL.min^{-1}$)	1345	1350
Pressure (MPa)	11.1	11.1
Dissolved Hydrogen ($cm^3.kg^{-1}$)	18	18
Dissolved Oxygen ($\mu g.kg^{-1}$)	<10	<10
Dissolved Cations* ($\mu g.kg^{-1}$):		
Co	<2.5	<2.5
Cr	<2.5	<2.5
Fe	<5.0	<5.0
Ni	<5.0	<5.0
Cu	<5.0	<5.0
Zn	0.4 - 37	0.6 - 16
Boron Concentration ($mg.kg^{-1}$)	1113 - 0	1113 - 0
Lithium Concentration ($mg.kg^{-1}$)	2.13 - 0.47	2.13 - 0.47

* from atomic absorption analysis

COOLANT CONDITIONS DURING ACTIVATION EXPERIMENT - PHASE 2

	TS 1	TS 2
Temperature (°C)	293	285
Flow Rate ($mL.min^{-1}$)	1290	1300
Pressure (MPa)	10.3	10.3
Dissolved Hydrogen ($cm^3.kg^{-1}$)	18	18
Dissolved Oxygen ($\mu g.kg^{-1}$)	<40	<40
Dissolved Cations* ($\mu g.kg^{-1}$):		
Co	<1.0	<1.0
Cr	<1.0	<1.0
Fe	<2.5	<2.5
Ni	<2.5	<2.5
Cu	<2.5	<2.5
Zn	6.5 - 17.0	0.3 - 0.7
Boron Concentration ($mg.kg^{-1}$)	1167 - 0	1167 - 0
Lithium Concentration ($mg.kg^{-1}$)	2.45 - 0.74	2.45 - 0.74
Cobalt-60 Concentration** ($\mu Ci.m^{-3}$)	2.17 - 16.62	2.17 - 16.62

* from atomic absorption analysis
** from gamma spectrometry of sample of combined TS flow after loop coolers.

Appendix A

Table A-2
Film Growth Rate on Alloy 600 Coupons During Phase 1 Tests of Lister (A-1)

	Release Rate, nM/h			
	TS1		TS2	
Time Period	No Zinc	Zinc	No Zinc	Zinc
0-517 h[a]	--	0.13	0.060	--
517-1034 h[b]	0.048	--	--	0.021
1034-1554 h[b]	--	0.096	0.019	--
1034-1554 h[c]	--	0.01	+0.01	--

a) Based on AES analyses

b) UWO database

c) AECL database

Table A-3
Equivalent Penetration Rates for Alloy 600 Based on Co-58 During Phase 1 Tests of Lister (A-1)

	Release Rate, nM/h			
	TS1		TS2	
Time Period	No Zinc	Zinc	No Zinc	Zinc
0-517 h	--	0.085	0.083	--
517-1034 h	0.054	--	--	0.033
1034-1554 h	--	0.0135	0.021	--

Table A-4
Film Growth Rate on Alloy 600 During Phase 2 Tests of Lister (X) (A-1)

	Film Growth Rate, nM/h	
Time	Zinc	No Zinc
0-1000 h	0.009	0.037
1000-1500 h	-0.006	-0.031
1500-2000 h	+0.007	+0.037
0-2012 h	0.005	0.021

Table A-5
Film Growth Rate on 304 Stainless Steel During Phase 2 Tests of Lister (A-1)[A]

		Film Thickness, nM	Rate, nM/h	Apparent Average Corrosion Rate, mg/dm^2-mo
T1	Zinc	307	0.152	3.6
	Zinc	347	0.172	4.2
T2	No Zinc	628	0.312	7.5
	No Zinc	486	0.242	5.7

a) 2012 h test period

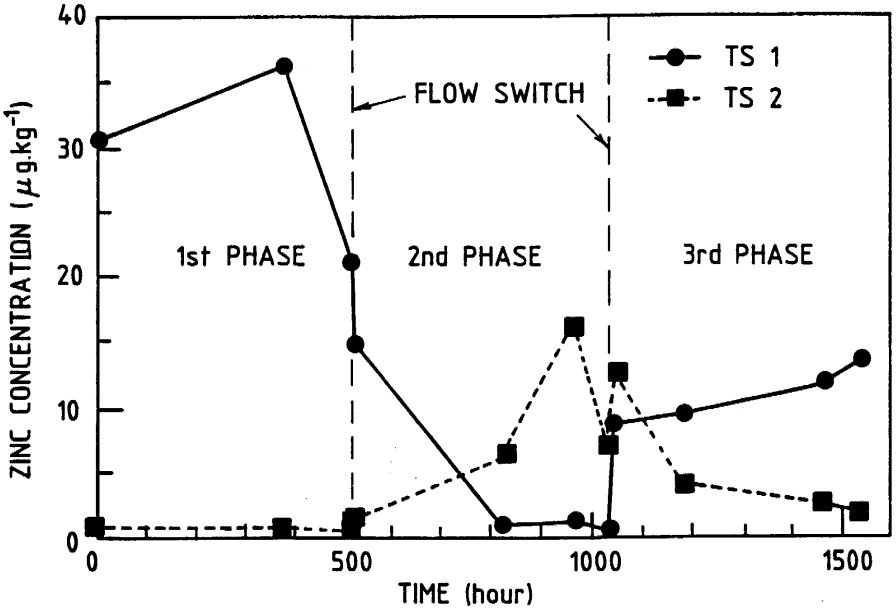

Figure A-1
Zinc Concentrations in Test Sections 1 and 2 During Release Experiment-Phase 1

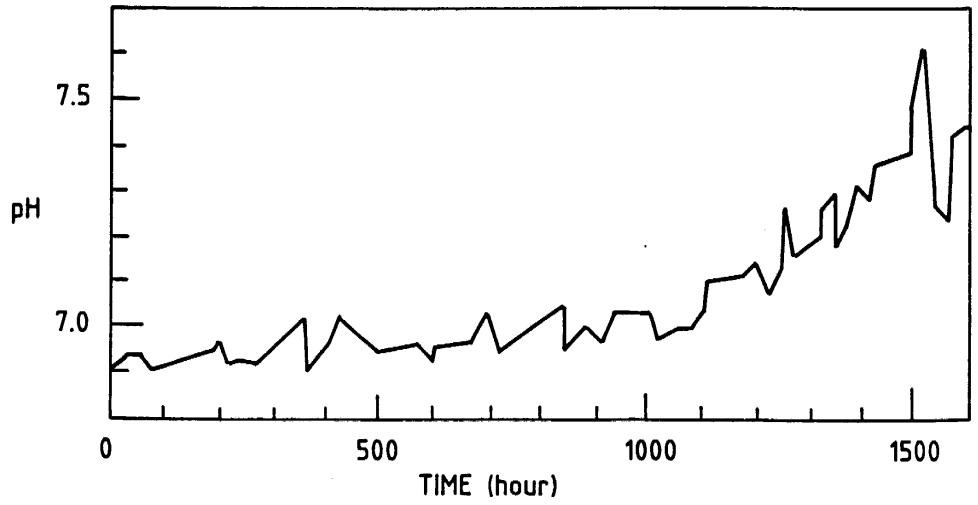

Figure A-2
High-Temperature pH of Coolant During Release Experiment-Phase 1

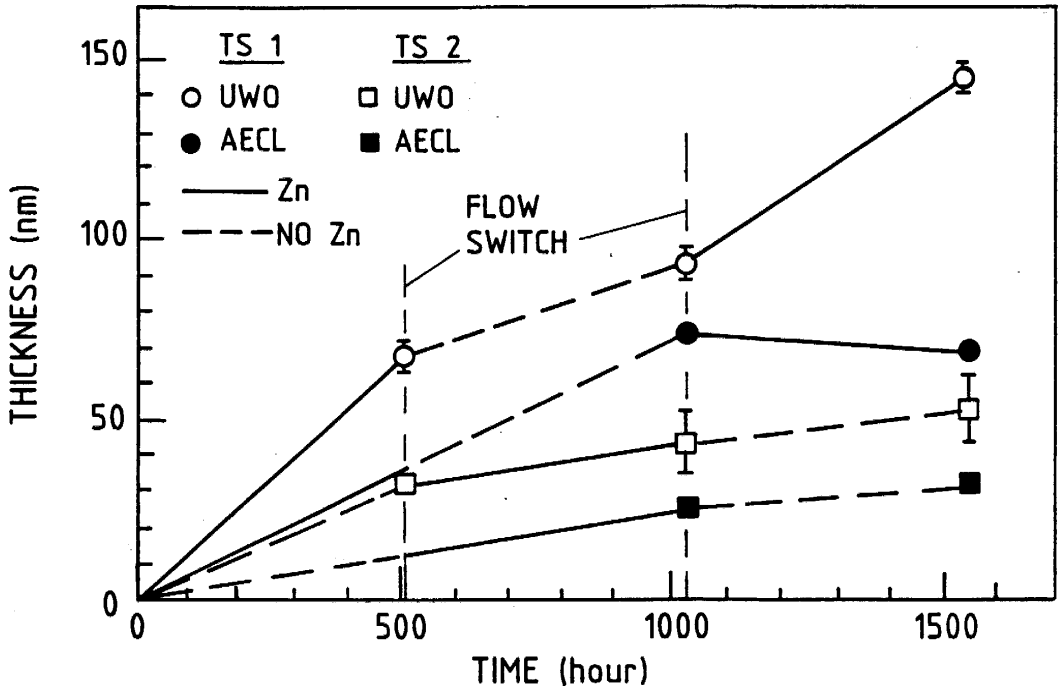

Figure A-3
Oxide Film Thickness on Inconel-600 in Simulated PWR CoolantWith and Without Zinc-Phase 1

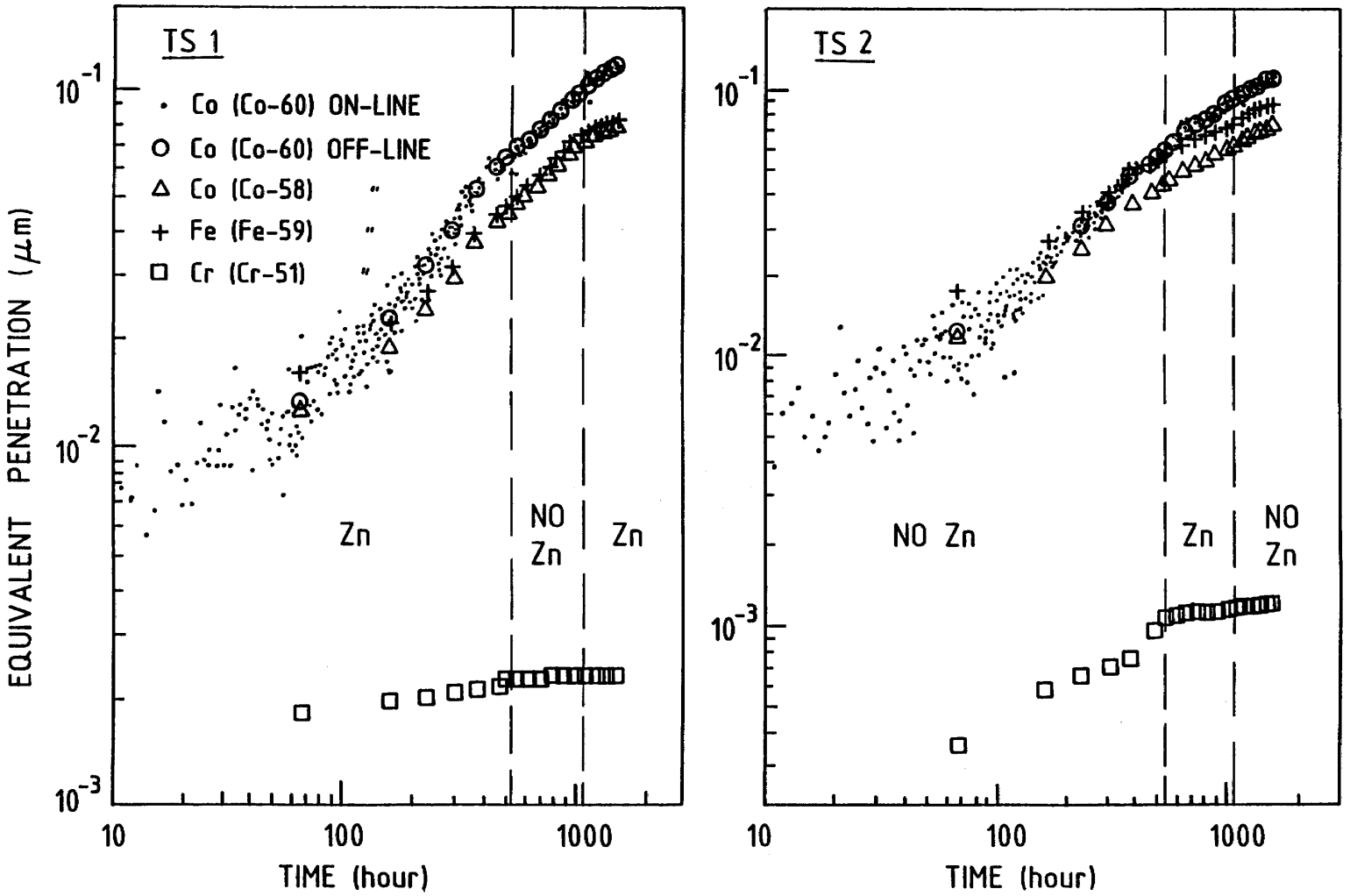

Figure A-4
Normalized Elemental Releases From Inconel-600 in Simulated PWR Coolant With and Without Zinc-Phase 1

Appendix A

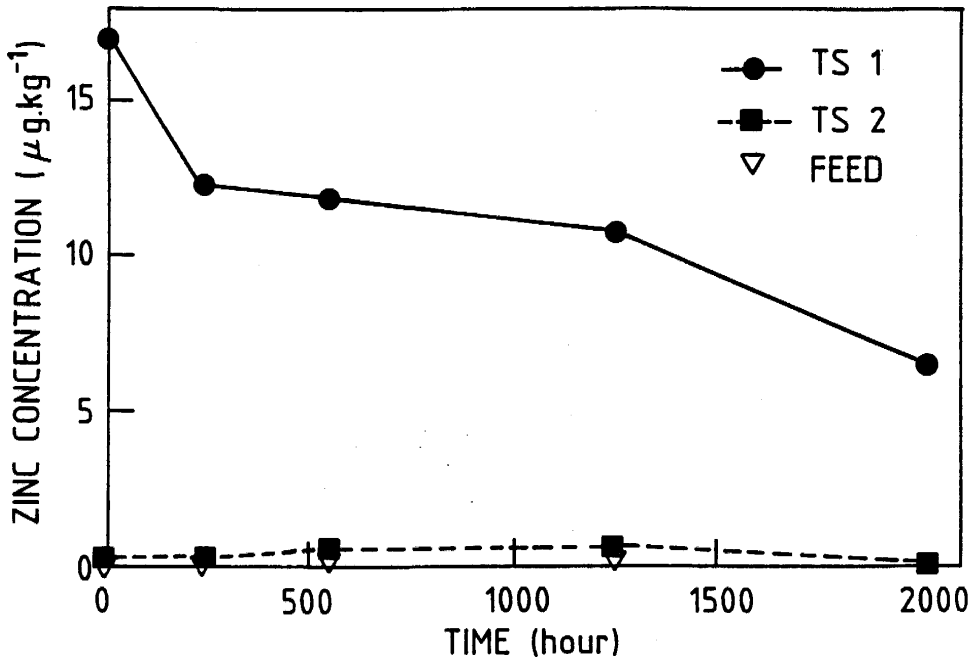

Figure A-5
Zinc Concentrations in Test Sections 1 and 2 During Activation Experiment-Phase 2

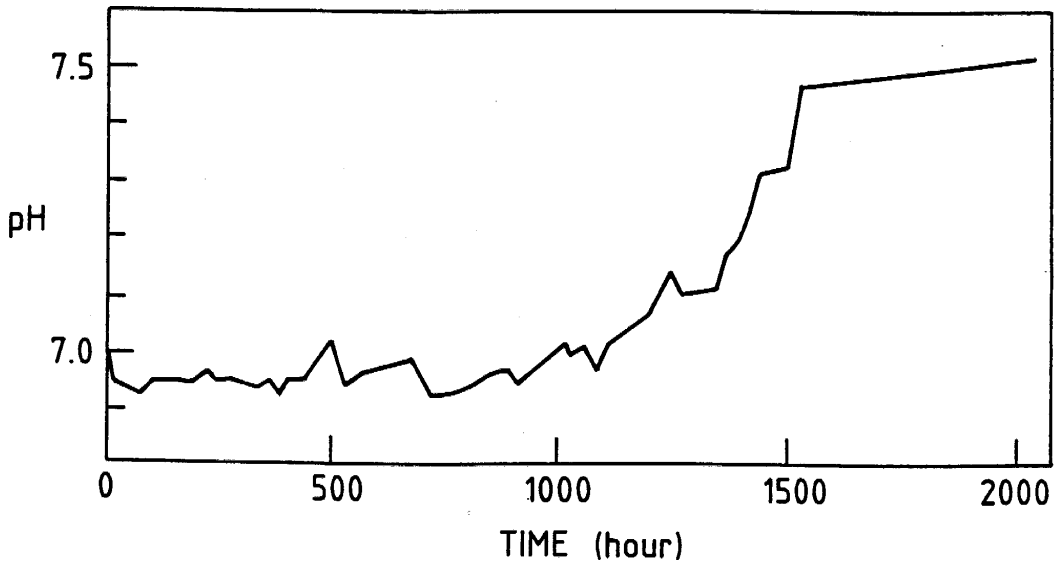

Figure A-6
High Temperature pH of Coolant During Activation Experiment-Phase 2

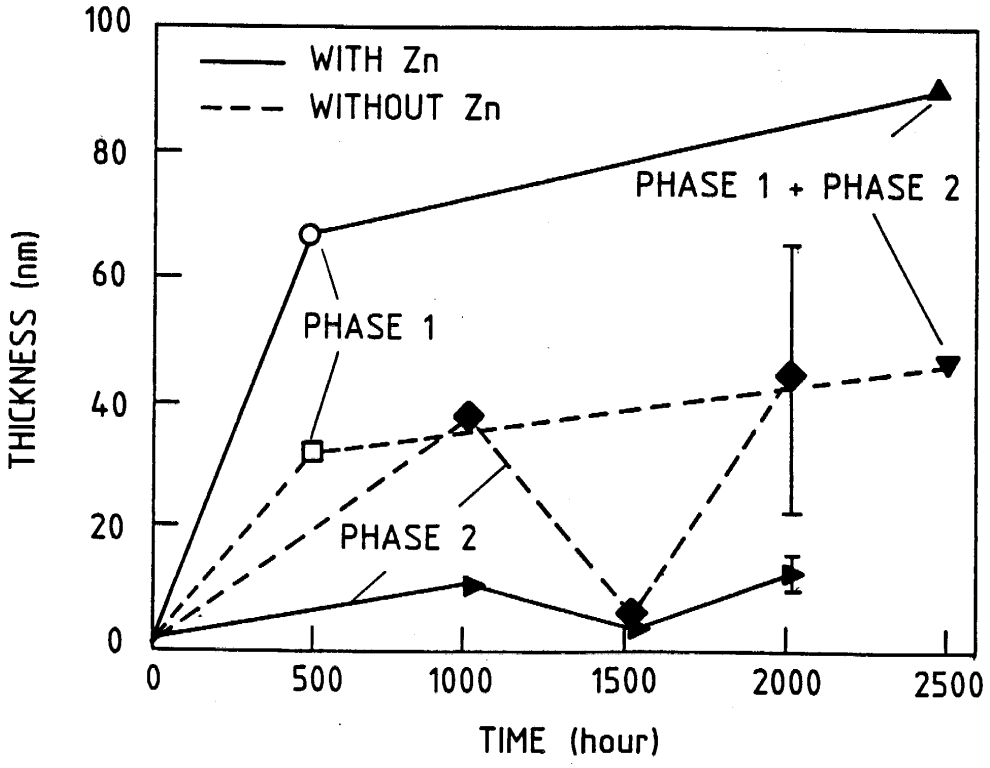

Figure A-7
Oxide Film Thickness on Inconel-600 in Simulated PWR Coolant With and Without Zinc

WARNING: This Document contains information classified under U.S. Export Control regulations as restricted from export outside the United States. You are under an obligation to ensure that you have a legal right to obtain access to this information and to ensure that you obtain an export license prior to any re-export of this information. Special restrictions apply to access by anyone that is not a United States citizen or a Permanent United States resident. For further information regarding your obligations, please see the information contained below in the section titled "Export Control Restrictions."

Export Control Restrictions

Access to and use of EPRI Intellectual Property is granted with the specific understanding and requirement that responsibility for ensuring full compliance with all applicable U.S. and foreign export laws and regulations is being undertaken by you and your company. This includes an obligation to ensure that any individual receiving access hereunder who is not a U.S. citizen or permanent U.S. resident is permitted access under applicable U.S. and foreign export laws and regulations. In the event you are uncertain whether you or your company may lawfully obtain access to this EPRI Intellectual Property, you acknowledge that it is your obligation to consult with your company's legal counsel to determine whether this access is lawful. Although EPRI may make available on a case by case basis an informal assessment of the applicable U.S. export classification for specific EPRI Intellectual Property, you and your company acknowledge that this assessment is solely for informational purposes and not for reliance purposes. You and your company acknowledge that it is still the obligation of you and your company to make your own assessment of the applicable U.S. export classification and ensure compliance accordingly. You and your company understand and acknowledge your obligations to make a prompt report to EPRI and the appropriate authorities regarding any access to or use of EPRI Intellectual Property hereunder that may be in violation of applicable U.S. or foreign export laws or regulations.

About EPRI

EPRI creates science and technology solutions for the global energy and energy services industry. U.S. electric utilities established the Electric Power Research Institute in 1973 as a nonprofit research consortium for the benefit of utility members, their customers, and society. Now known simply as EPRI, the company provides a wide range of innovative products and services to more than 1000 energy-related organizations in 40 countries. EPRI's multidisciplinary team of scientists and engineers draws on a worldwide network of technical and business expertise to help solve today's toughest energy and environmental problems.

EPRI. Electrify the World

SINGLE USER LICENSE AGREEMENT

THIS IS A LEGALLY BINDING AGREEMENT BETWEEN YOU AND THE ELECTRIC POWER RESEARCH INSTITUTE, INC. (EPRI). PLEASE READ IT CAREFULLY BEFORE REMOVING THE WRAPPING MATERIAL.

BY OPENING THIS SEALED PACKAGE YOU ARE AGREEING TO THE TERMS OF THIS AGREEMENT. IF YOU DO NOT AGREE TO THE TERMS OF THIS AGREEMENT, PROMPTLY RETURN THE UNOPENED PACKAGE TO EPRI AND THE PURCHASE PRICE WILL BE REFUNDED.

1. GRANT OF LICENSE

EPRI grants you the nonexclusive and nontransferable right during the term of this agreement to use this package only for your own benefit and the benefit of your organization. This means that the following may use this package: (I) your company (at any site owned or operated by your company); (II) its subsidiaries or other related entities; and (III) a consultant to your company or related entities, if the consultant has entered into a contract agreeing not to disclose the package outside of its organization or to use the package for its own benefit or the benefit of any party other than your company.

This shrink-wrap license agreement is subordinate to the terms of the Master Utility License Agreement between most U.S. EPRI member utilities and EPRI. Any EPRI member utility that does not have a Master Utility License Agreement may get one on request.

2. COPYRIGHT

This package, including the information contained in it, is either licensed to EPRI or owned by EPRI and is protected by United States and international copyright laws. You may not, without the prior written permission of EPRI, reproduce, translate or modify this package, in any form, in whole or in part, or prepare any derivative work based on this package.

3. RESTRICTIONS

You may not rent, lease, license, disclose or give this package to any person or organization, or use the information contained in this package, for the benefit of any third party or for any purpose other than as specified above unless such use is with the prior written permission of EPRI. You agree to take all reasonable steps to prevent unauthorized disclosure or use of this package. Except as specified above, this agreement does not grant you any right to patents, copyrights, trade secrets, trade names, trademarks or any other intellectual property, rights or licenses in respect of this package.

4. TERM AND TERMINATION

This license and this agreement are effective until terminated. You may terminate them at any time by destroying this package. EPRI has the right to terminate the license and this agreement immediately if you fail to comply with any term or condition of this agreement. Upon any termination you may destroy this package, but all obligations of nondisclosure will remain in effect.

5. DISCLAIMER OF WARRANTIES AND LIMITATION OF LIABILITIES

NEITHER EPRI, ANY MEMBER OF EPRI, ANY COSPONSOR, NOR ANY PERSON OR ORGANIZATION ACTING ON BEHALF OF ANY OF THEM:

(A) MAKES ANY WARRANTY OR REPRESENTATION WHATSOEVER, EXPRESS OR IMPLIED, (I) WITH RESPECT TO THE USE OF ANY INFORMATION, APPARATUS, METHOD, PROCESS OR SIMILAR ITEM DISCLOSED IN THIS PACKAGE, INCLUDING MERCHANTABILITY AND FITNESS FOR A PARTICULAR PURPOSE, OR (II) THAT SUCH USE DOES NOT INFRINGE ON OR INTERFERE WITH PRIVATELY OWNED RIGHTS, INCLUDING ANY PARTY'S INTELLECTUAL PROPERTY, OR (III) THAT THIS PACKAGE IS SUITABLE TO ANY PARTICULAR USER'S CIRCUMSTANCE; OR

(B) ASSUMES RESPONSIBILITY FOR ANY DAMAGES OR OTHER LIABILITY WHATSOEVER (INCLUDING ANY CONSEQUENTIAL DAMAGES, EVEN IF EPRI OR ANY EPRI REPRESENTATIVE HAS BEEN ADVISED OF THE POSSIBILITY OF SUCH DAMAGES) RESULTING FROM YOUR SELECTION OR USE OF THIS PACKAGE OR ANY INFORMATION, APPARATUS, METHOD, PROCESS OR SIMILAR ITEM DISCLOSED IN THIS PACKAGE.

6. EXPORT

The laws and regulations of the United States restrict the export and re-export of any portion of this package, and you agree not to export or re-export this package or any related technical data in any form without the appropriate United States and foreign government approvals.

7. CHOICE OF LAW

This agreement will be governed by the laws of the State of California as applied to transactions taking place entirely in California between California residents.

8. INTEGRATION

You have read and understand this agreement, and acknowledge that it is the final, complete and exclusive agreement between you and EPRI concerning its subject matter, superseding any prior related understanding or agreement. No waiver, variation or different terms of this agreement will be enforceable against EPRI unless EPRI gives its prior written consent, signed by an officer of EPRI.

1001396

© 2001 Electric Power Research Institute (EPRI), Inc. All rights reserved. Electric Power Research Institute and EPRI are registered service marks of the Electric Power Research Institute, Inc. EPRI. ELECTRIFY THE WORLD is a service mark of the Electric Power Research Institute, Inc.

Printed on recycled paper in the United States of America

EPRI • 3412 Hillview Avenue, Palo Alto, California 94304 • PO Box 10412, Palo Alto, California 94303 • USA
800.313.3774 • 650.855.2121 • askepri@epri.com • www.epri.com